The Astronomical Journal, 141:144 (9pp), 2011 May doi:10.1088/0004-6256/141/5/144

OBSERVATIONS AND ORBITAL ANALYSIS OF THE GIANT WHITE DWARF BINARY SYSTEM HR 5692

Robert P. Stefanik[1], Guillermo Torres[1], David W. Latham[1],
Wayne Landsman[2], Nathaniel Craig[3], and James Murrett[3]
[1] Harvard-Smithsonian Center for Astrophysics, 60 Garden Street, Cambridge, MA 02138, USA
[2] NASA Goddard Space Flight Center, Greenbelt, MD 20771, USA
[3] Harvard College, Cambridge, MA 02138, USA; rstefanik@cfa.harvard.edu
Received 2010 December 15; accepted 2011 February 11; published 2011 March 22

ABSTRACT

We report spectroscopic observations of the red giant star HR 5692, previously known to be a binary system both from other spectroscopic work and from deviations in the astrometric motion detected by the *Hipparcos* satellite. Earlier *International Ultraviolet Explorer* (*IUE*) observations had shown the presence of a hot white dwarf companion to the giant primary. We have combined our radial velocity observations with other existing measurements and with the *Hipparcos* intermediate astrometric data to determine a complete astrometric-spectroscopic orbital solution, providing the inclination angle for the first time. We also determine an improved parallax for the system of 10.12 ± 0.67 mas. We derive the physical properties of the primary, and with an estimate of its mass from stellar evolution models ($1.84 \pm 0.40\ M_{\odot}$), we infer the mass of the white dwarf companion to be $M_{\rm WD} = 0.59 \pm 0.12\ M_{\odot}$. An analysis of an *IUE* white dwarf spectrum, using our parallax, yields $T_{\rm eff} = 30{,}400 \pm 780$ K, $\log g = 8.25 \pm 0.15$, and a mass $M_{\rm WD} = 0.79 \pm 0.09\ M_{\odot}$, in marginal agreement with the dynamical mass.

Key words: binaries: general – methods: data analysis – stars: individual (HR 5692) – techniques: spectroscopic – white dwarfs

1. INTRODUCTION

Historically, the red giant HR 5692 (HD 136138, HIP 74896, $V = 5.70$) had been an unremarkable member of the stellar community. For some time it was thought to be a weak barium star (Lu 1991) and therefore probably a binary system since all barium stars are in binary systems (McClure & Woodsworth 1990). However, Jorissen et al. (1996) report that the X-ray properties of HR 5692, along with its normal photometric indices and weak chemical peculiarities, suggest that the star is a coronal X-ray source and might not be a barium star. Nevertheless, several other lines of evidence show that the star is indeed a binary system. Based on radial velocity observations, the star was identified as a spectroscopic binary by de Medeiros & Mayor (1999). In addition, the *Hipparcos* mission (Perryman et al. 1997) detected significant acceleration in the astrometric motion of HR 5692, which required including terms representing first and second derivatives of the proper-motion components in order to properly model the trajectory on the plane of the sky (*Hipparcos* Double and Multiple System Annex; see also Makarov & Kaplan 2005). Such accelerations are a strong suggestion that HR 5692 is a binary system whose unaccounted orbital motions give rise to the observed deviations. Frankowski et al. (2007) flagged it as a proper-motion binary by comparing the *Hipparcos* proper motion with the *Tycho-2* proper motion. Orbital solutions based only on radial velocity observations have been given more recently by Massarotti et al. (2008) and Griffin (2009). Attempts to resolve the binary using speckle interferometry have been unsuccessful (Mason et al. 1999).

Further evidence for the binary nature of HR 5692 comes from unpublished data from the *International Ultraviolet Explorer* (*IUE*), examined some years ago by one of the present authors. Strong UV flux and broad Lyα absorption in the *IUE* UV spectrum, shown in Figure 1, indicate the presence of a hot white dwarf companion to the primary, with the giant primary dominating only the optical wavelengths and the much hotter secondary being evident at ultraviolet wavelengths. From the UV spectrum and using the *Hipparcos* distance of 89 pc, an estimate of 28,000 K was made for the white dwarf's temperature, and a mass of $0.88\ M_{\odot}$ was inferred. Since a typical white dwarf mass is close to $\sim 0.6\ M_{\odot}$, a value as large as $0.88\ M_{\odot}$ seems uncommonly high.

The dynamical information provided by the published spectroscopic orbits has so far been of limited help because the inclination angle of the orbit remained unknown. The detection of acceleration on the plane of the sky by *Hipparcos* offers the possibility of extracting the inclination angle from those measurements, allowing the mass of the companion to be determined if a reliable estimate of the primary mass can be made. With this as one of our motivations for this paper, we begin by presenting the results of our new radial velocity monitoring of HR 5692 which, along with previous radial velocity data, yields an updated spectroscopic orbit. We then model the physical properties of the primary star using our spectra and current stellar evolution models. The radial velocities, when combined with the *Hipparcos* intermediate data, allow for a complete spectroscopic-astrometric orbital solution that provides the first dynamically based determination of the absolute mass of the white dwarf companion.

As a second goal, in Section 5 we give a re-analysis of the *IUE* spectrum of HR 5692 using our revised parallax (Section 3) and reddening determination (Section 4) to derive an estimate of the white dwarf temperature and another estimate of its mass. Possible formation scenarios for this system are discussed briefly in Section 6.

2. SPECTROSCOPIC OBSERVATIONS AND REDUCTIONS

HR 5692 was observed between 2003 December and 2009 February with the CfA Digital Speedometers (Latham 1985, 1992) at the 1.5 m Wyeth Reflector at the Oak Ridge Observatory (Harvard, MA) and the 1.5 m Tillinghast Reflector at the

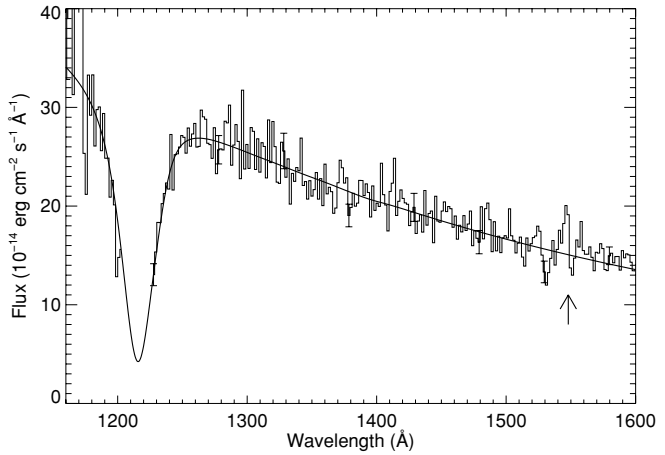

Figure 1. *IUE* spectrum of HR 5692 overlayed with a model white dwarf spectrum with $\log g = 8.0$ and $T_{\rm eff} = 29{,}431$ K. The arrow points to a weak feature near 1548 Å which may be due to C IV emission.

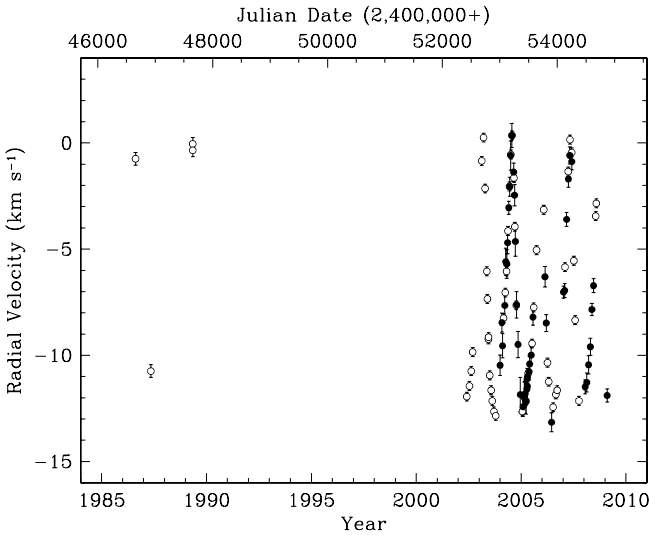

Figure 2. Time history of the radial velocities of HR 5692. Filled circles correspond to CfA observations, and open circles to measurements from Griffin (2009).

F. L. Whipple Observatory (Mt. Hopkins, AZ). Two nearly identical echelle spectrographs were used, with photon-counting intensified Reticon detectors that recorded about 45 Å of spectrum in a single order centered at 5187 Å. The resolving power is $\lambda/\Delta\lambda \approx 35{,}000$, and the signal-to-noise ratios of our 45 Å spectra range from about 17 to 67 per resolution element of 8.5 km s^{-1}.

Radial velocities were extracted using the one-dimensional cross-correlation task `XCSAO` (Kurtz & Mink 1998) running under IRAF.[4] We used templates from a large library of synthetic spectra computed for us by John Laird using a line list developed by Jon Morse and model atmospheres by R. L. Kurucz[5] (see Nordström et al. 1994). These calculated spectra cover a wide range in effective temperature ($T_{\rm eff}$), rotational velocity (interpreted as the projected $v \sin i$), surface gravity ($\log g$), and metallicity ([m/H]). The stability of the zero point of our velocity system was monitored by means of exposures of the dusk and dawn sky, and small systematic run-to-run corrections were applied in the manner described by Latham (1992).

The optimum synthetic template for HR 5692 was determined from grids of cross-correlations, initially over a range of temperatures and rotational velocities, which are the parameters that affect the velocities the most (see, e.g., Torres et al. 2002). Surface gravity and metallicity are strongly correlated with temperature. We therefore assumed a fixed value of $\log g = 2.5$ (see below) and solar composition to begin with, guided by the various abundance determinations for the star averaging [Fe/H] = −0.21 (see Section 4). The template parameters giving the highest correlation averaged over all exposures were $T_{\rm eff} = 5000$ K and $v \sin i = 8$ km s^{-1}, which we adopted for determining the radial velocities.[6] Small changes in these parameters have little effect on the velocities.

In order to derive the atmospheric properties of the primary star, we ran additional sets of cross-correlations in which we repeated the above grids varying the surface gravity, and we did this for solar composition and also for [m/H] = −0.5, bracketing the abundance determinations reported in the literature. By interpolation to [m/H] = −0.21 we then determined the temperature and gravity of HR 5692 to be $T_{\rm eff} = 4960 \pm 100$ K and $\log g = 2.67 \pm 0.20$, respectively.

We list the CfA heliocentric radial velocities in Table 1. The velocities published by Massarotti et al. (2008) are based on a subset of the same spectra used here, and are thus superseded by the present reductions. The time history of the radial-velocity measurements of HR 5692 is shown in Figure 2. Also shown in this figure are the radial velocity measurements reported by Griffin (2009), which, in addition to his Cambridge observations obtained between 2002 and 2008, include four observations made prior to 1990 by de Medeiros & Mayor (1999) at the Haute Provence Observatory. Those measurements extend the time coverage considerably, as seen in the figure. All of these additional observations have been adjusted slightly to bring them onto the CfA native velocity system, as described in the next section.

3. COMBINED ORBITAL SOLUTION

The detection of significant acceleration in the motion of HR 5692 by *Hipparcos* is a clear indication that the perturbation by the companion was detected in those measurements, which have a typical precision (median error) of 2.4 mas for this star. A total of 70 measurements were derived by the two independent data reduction consortia (see Perryman et al. 1997) based on the one-dimensional scans performed by the satellite over a period of three years. Given that the light contributed by the white dwarf is negligible, the measurements refer strictly to the motion of the primary around the center of mass of the binary. Here, we use those individual astrometric measurements (referred to in the *Hipparcos* catalog as "abscissa residuals") in combination with our radial velocity data and those of Griffin (2009) to derive an astrometric-spectroscopic orbital solution for the system. The information provided by *Hipparcos* allows us to derive the inclination angle of the orbit, which is one of the key missing ingredients to infer the mass of the white dwarf companion.

[4] IRAF (Image Reduction and Analysis Facility) is distributed by the National Optical Astronomy Observatories, which are operated by the Association of Universities for Research in Astronomy, Inc., under contract with the National Science Foundation.

[5] Available at http://kurucz.harvard.edu.

[6] Our $v \sin i$ estimate as derived here represents a measure of the total line broadening in our spectra. The actual rotational broadening may be smaller if other broadening sources such as macroturbulence are larger than assumed in our templates, which are designed for dwarfs. Massarotti et al. (2008) studied the effects of macroturbulence and stellar rotation on spectral line broadening of giant stars, and reported for HR 5692 an observed spectral line broadening of 8.5 km s^{-1} and a derived projected rotational velocity of 7.7 km s^{-1}.

Table 1
Heliocentric Radial Velocities from CfA for HR 5692

Date (HJD −2,400,000)	Year	Phase	RV (km s^{-1})	σ_{RV}[a] (km s^{-1})	$O-C$ (km s^{-1})
53004.9618	2003.9972	0.5353	−10.47	0.48	+0.32
53035.8918	2004.0818	0.5964	−8.46	0.45	+1.35
53046.8325	2004.1118	0.6180	−9.55	0.57	−0.14
53086.7758	2004.2212	0.6969	−7.65	0.60	−0.01
53102.7068	2004.2648	0.7283	−5.59	0.64	+1.20
53120.7011	2004.3140	0.7638	−5.70	0.67	+0.01
53135.7468	2004.3552	0.7936	−4.70	0.52	+0.01
53155.6320	2004.4097	0.8328	−3.05	0.31	+0.22
53170.6434	2004.4508	0.8625	−2.06	0.45	+0.06
53188.6459	2004.5001	0.8980	−0.59	0.69	+0.23
53207.6480	2004.5521	0.9355	+0.35	0.57	+0.23
53240.5699	2004.6422	0.0005	−1.37	0.43	−0.42
53255.5106	2004.6831	0.0300	−2.46	0.50	+0.29
53271.4828	2004.7269	0.0616	−4.64	0.69	+0.38
53291.4556	2004.7815	0.1010	−7.62	0.62	+0.01
53316.4322	2004.8499	0.1503	−9.49	0.62	+0.47
53355.9690	2004.9582	0.2284	−11.85	0.81	−0.01
53403.9678	2005.0896	0.3232	−12.42	0.45	+0.01
53425.8438	2005.1495	0.3664	−12.00	0.74	+0.35
53440.8185	2005.1905	0.3959	−11.81	0.60	+0.40
53456.8386	2005.2343	0.4276	−12.19	0.57	−0.20
53471.6910	2005.2750	0.4569	−11.59	0.52	+0.14
53474.6498	2005.2831	0.4627	−11.11	0.50	+0.56
53480.6543	2005.2995	0.4746	−11.46	0.60	+0.09
53480.7579	2005.2998	0.4748	−11.01	0.29	+0.54
53508.8089	2005.3766	0.5302	−10.77	0.38	+0.10
53517.8102	2005.4013	0.5480	−10.41	0.36	+0.20
53546.7195	2005.4804	0.6050	−9.99	0.40	−0.33
53576.6879	2005.5625	0.6642	−8.20	0.38	+0.23
53785.9838	2006.1355	0.0775	−6.30	0.48	−0.16
53807.9834	2006.1957	0.1209	−8.48	0.40	+0.21
53900.7391	2006.4497	0.3041	−13.15	0.45	−0.74
54109.0516	2007.0200	0.7154	−7.02	0.29	+0.13
54130.0637	2007.0775	0.7569	−6.95	0.33	−1.01
54163.0157	2007.1677	0.8219	−3.60	0.33	+0.08
54193.9117	2007.2523	0.8829	−1.70	0.38	−0.35
54217.8179	2007.3178	0.9301	−0.59	0.40	−0.63
54251.8248	2007.4109	0.9973	−0.88	0.38	−0.08
54485.0760	2008.0495	0.4578	−11.49	0.33	+0.23
54514.0671	2008.1289	0.5151	−11.28	0.45	−0.21
54544.9260	2008.2133	0.5760	−10.45	0.43	−0.28
54575.9034	2008.2982	0.6372	−9.60	0.40	−0.58
54602.8081	2008.3718	0.6903	−7.84	0.29	−0.03
54631.7803	2008.4511	0.7475	−6.72	0.33	−0.49
54869.0566	2009.1008	0.2160	−11.89	0.31	−0.23

Note. [a] Errors include the scale factor described in the text.

The orbital elements on which the radial velocities provide information are as usual the period (P), center-of-mass velocity (γ), velocity semi-amplitude (K), eccentricity (e), longitude of periastron (ω), and time of periastron passage (T). The astrometric observations constrain the inclination angle (i), the position angle of the ascending node (Ω, J2000), and the angular scale of the orbit of the red giant primary (a''_{RG}). Five additional parameters come into play because of the fact that the *Hipparcos* observations were made in an absolute frame of reference. Those quantities represent corrections to the catalog values of the position and proper motion of the barycenter ($\Delta\alpha^*$, $\Delta\delta$, $\Delta\mu^*_\alpha$, $\Delta\mu_\delta$)[7] and a correction to the trigonometric parallax of the system ($\Delta\pi_{HIP}$).

[7] Following the practice of the *Hipparcos* catalog, we define $\Delta\alpha^* \equiv \Delta\alpha\cos\delta$ and $\Delta\mu^*_\alpha \equiv \Delta\mu_\alpha\cos\delta$.

Both the spectroscopy and the astrometry constrain the semimajor axis of the primary (in either linear or angular units). We may exploit this redundancy to eliminate a''_{RG} as one of the unknowns since it may be expressed in terms of other elements as

$$a''_{RG} = 9.191967\times10^{-5}\cdot\pi_{HIP}KP\sqrt{1-e^2}/\sin i, \quad (1)$$

where K is given in units of km s^{-1} and P in days. One additional parameter, ΔRV, was added to account for the possible offset between the zero points of the radial velocities of Griffin (2009) compared to CfA. Thus, we are left with 14 adjustable parameters, which we solved for using standard nonlinear least-squares techniques (Press et al. 1992, p. 650). The formalism used to incorporate the abscissa residuals from *Hipparcos* into the fit closely follows that described by van Leeuwen & Evans

Table 2
Orbital Elements for HR 5692

Parameter	Combined Solution
Adjusted quantities	
P (days)	506.45 ± 0.18
γ (km s^{-1})	−7.826 ± 0.065
K (km s^{-1})	6.340 ± 0.044
ΔRV (km s^{-1}) [Griffin−CfA]	−1.043 ± 0.073
e	0.3353 ± 0.0056
ω (deg)	35.4 ± 1.2
T (HJD−2,400,000)	53240.3 ± 1.3
i (deg)	42.9 ± 6.7
Ω (deg)	207.0 ± 7.4
$\Delta\alpha^*$ (mas)	−2.56 ± 0.50
$\Delta\delta$ (mas)	+2.09 ± 0.56
$\Delta\mu_\alpha^*$ (mas yr^{-1})	+3.00 ± 0.65
$\Delta\mu_\delta$ (mas yr^{-1})	−7.28 ± 0.73
$\Delta\pi_{\rm HIP}$ (mas)	−1.11 ± 0.67
Derived quantities	
$a''_{\rm RG}$ (mas)	4.14 ± 0.52
μ_α^* (mas yr^{-1})	−11.57 ± 0.65
μ_δ (mas yr^{-1})	−20.41 ± 0.73
$\pi_{\rm HIP}$ (mas)	10.12 ± 0.67
Other quantities pertaining to the fit	
$\sigma_{\rm RV}$ CfA (km s^{-1})	0.43
$\sigma_{\rm RV}$ Griffin (km s^{-1})	0.22
$\sigma_{\rm HIP}$ (mas)	3.62
$N_{\rm RV}$ CfA	45
$N_{\rm RV}$ Griffin	51
$N_{\rm HIP}$	70
Time span (yr)	22.5
Time span (orbital cycles)	16.2

Table 3
Comparison of Astrometric Parameters for HR 5692

Parameter	*Hipparcos*	*Tycho-2*	Combined Solution
μ_α^* (mas yr^{-1})	−14.57 ± 1.55	−12.6 ± 0.6	−11.57 ± 0.65
μ_δ (mas yr^{-1})	−13.13 ± 1.70	−20.4 ± 0.6	−20.41 ± 0.73
$\pi_{\rm HIP}$ (mas)	11.23 ± 0.85	...	10.12 ± 0.67

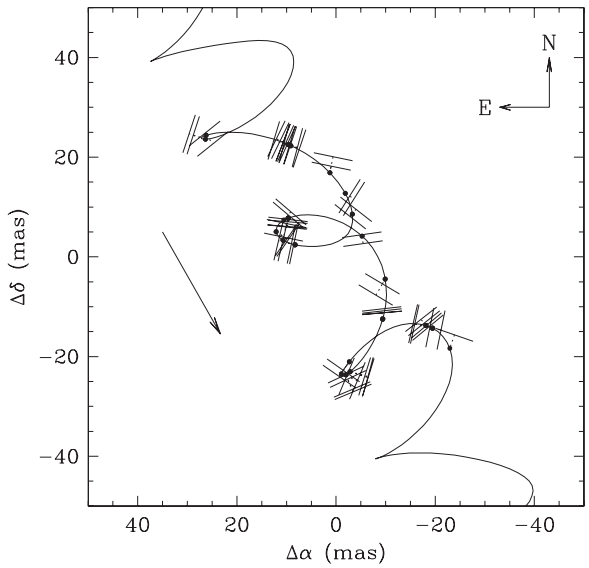

Figure 3. Path of HR 5692 on the plane of the sky, resulting from the combination of proper motion, parallactic motion, and orbital motion. The one-dimensional *Hipparcos* observations are represented schematically as described in the text. A few large residuals have been omitted for clarity. The arrow indicates the magnitude and direction of the annual proper motion.

(1998) and Pourbaix & Jorissen (2000), and another example of a similar application may be seen in the work of Torres (2007).

Initial errors for the CfA velocities were taken as reported by the XCSAO correlation task. Individual weights for the Griffin (2009) observations were adopted as published, and an observation of unit weight for this data set was initially assigned an error of 0.2 km s^{-1}. The *Hipparcos* uncertainties were also taken as published. Since internal observational errors are not always realistic, the relative weighting between the two separate velocity data sets and the astrometric measurements was established by iterations, in such a way as to produce a reduced χ^2 near unity for each type of observation. In this way, we determined scale factors for the original internal errors of 2.38 for the CfA velocities, 1.07 for those of Griffin (2009), and 1.16 for the abscissa residuals.

The elements of our astrometric-spectroscopic solution are given in Table 2 along with other derived quantities. The new parallax corresponds to a distance of $98.8^{+7.0}_{-6.1}$ pc. Velocity residuals are listed in Table 1. As anticipated, we note that the revised proper motion components for HR 5692 are significantly different from the *Hipparcos* values, a result of our properly accounting for the motion in the binary. Table 3 lists both determinations for comparison purposes. Also listed is the proper motion from the *Tycho-2* catalog (Høg et al. 2000). While the *Hipparcos* determination is effectively "instantaneous" (based on observations covering only three years), the *Tycho-2* value is based on ground-based positional measurements going back nearly a century in some cases, and is constrained at the recent epoch by the *Tycho-2* position. Consequently, any binary motion with a period significantly shorter than this baseline is averaged out, and the result should be more reliable than *Hipparcos*. Indeed, Table 3 shows that our measurement is much closer to *Tycho-2* than *Hipparcos*. We also note that our revised parallax is slightly smaller than the *Hipparcos* value (Perryman et al. 1997), as well as somewhat more precise. This original parallax estimate by the *Hipparcos* team is based on a nine-parameter description of the astrometric motion (position, parallax, proper motion components, and first and second derivatives of the proper motions; see Section 1). A new reduction of the *Hipparcos* data was performed by van Leeuwen (2007), and the parallax value reported there is $\pi_{\rm HIP} = 9.15 \pm 0.65$ mas, slightly ($\sim 1\sigma$) smaller than ours. However, for this reduction the author reverted to a "stochastic" solution for HR 5692, i.e., a simple five-parameter fit for parallax, position, and proper motion components (rather than a nine-parameter solution, as in the original catalog) in which the excess scatter in the amount of 2.3 mas was considered simply as "cosmic dispersion." Nonlinear motion (aside from the parallactic displacement) was not modeled, as we have done here, and the result is therefore suspect.

Figure 3 illustrates the path of HR 5692 on the plane of the sky, along with a schematic representation of the *Hipparcos* measurements. The axes are parallel to the right ascension and declination directions. The curious pattern of the curve is the result of the combined effects of annual parallax, proper motion, and orbital motion. The largest contribution is from the proper motion (23.5 mas yr^{-1}), which is indicated with an arrow, followed by the parallactic (10 mas) and orbital (4 mas) components. Because they are one-dimensional in nature (Perryman et al. 1997), the exact location of each *Hipparcos* measurement on the plane of the sky is difficult to show graphically. In Figure 3, we have used filled circles

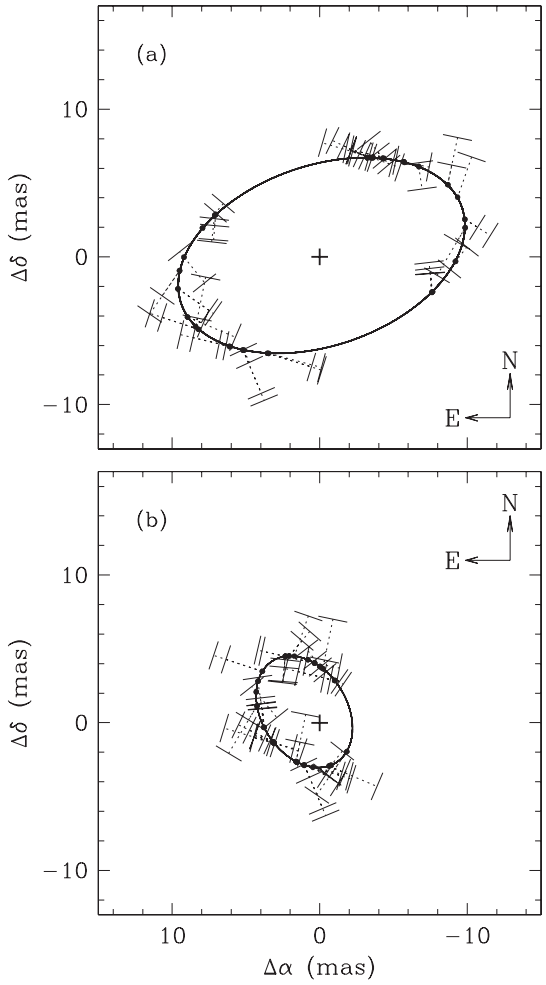

Figure 4. Separate components of the motion of HR 5692 on the plane of the sky. The one-dimensional *Hipparcos* observations are represented as in Figure 3. (a) Parallactic motion after removal of proper motion and orbital motion; (b) orbital motion relative to the center of mass of the binary, on the same scale as the top panel.

to indicate the predicted location of each measurement on the computed orbit. The dotted lines connecting to each filled circle indicate the scanning direction of the *Hipparcos* satellite for each observation, and show which side of the orbit the residual is on. The short line segments at the end of and perpendicular to the dotted lines indicate the direction along which the actual observation lies, although the precise location is undetermined. Occasionally, more than one measurement was taken along the same scanning direction, in which case two or more short line segments appear on the same dotted lines.

In Figure 4(a), we have subtracted the proper motion and orbital motion, leaving only the effect of annual parallax. Figure 4(b) represents the orbital motion on the same scale as before, after removing the proper motion and the annual parallax. Finally, the radial velocity observations along with the computed orbit are shown in Figure 5, phased with the orbital period. Residuals are displayed in the lower panel.

4. PHYSICAL PROPERTIES OF THE COMPONENTS

With a complete set of orbital elements we are in a position to determine the mass of the white dwarf companion, provided we can obtain an estimate of the mass of the red giant primary. For this we rely on the location of the star in the H-R diagram

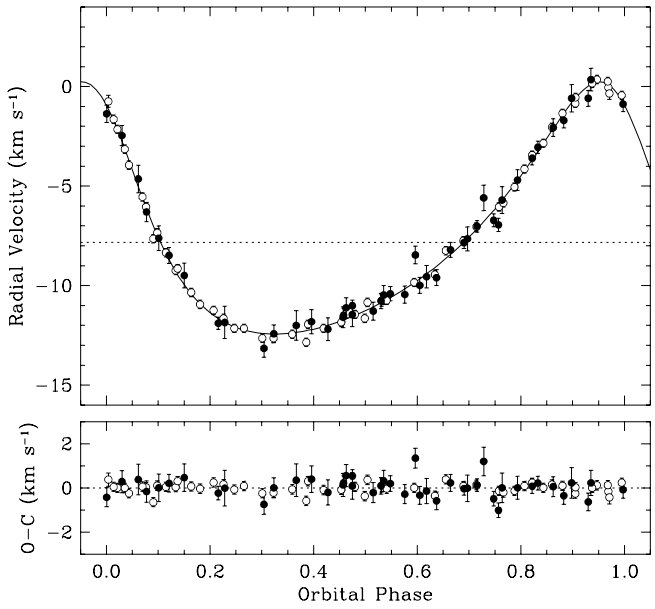

Figure 5. Radial velocity observations of HR 5692 phased with the orbital period, along with the computed orbit from our combined solution. Filled circles correspond to CfA and open circles to the observations by Griffin (2009), adjusted to place them on the CfA zero point. The center-of-mass velocity is represented by the dotted line. The bottom panel displays the $O-C$ residuals.

and a comparison with stellar evolution models. The physical properties of the giant required for this comparison are described below.

The metallicity of the star has been measured by several authors. Brown et al. (1989) reported a spectroscopic determination of [Fe/H] = −0.24 (no error given), as well as a photometric index δCN = −0.018 from the DDO system leading to an additional estimate of [Fe/H] = −0.19. The spectroscopic study by Mishenina et al. (2006) gave [Fe/H] = −0.19 ± 0.13. There is good agreement among these values, and in the following we adopt an average of [Fe/H] = −0.21 ± 0.05.

The absolute visual magnitude of HR 5692 follows from the apparent magnitude ($V = 5.700 \pm 0.009$; Häggkvist & Oja 1987) and our revised parallax ($\pi_{\rm HIP} = 10.12 \pm 0.67$ mas; Section 3). Although there is no reason to expect significant interstellar extinction, examination of the dust maps by Schlegel et al. (1998) in the direction of HR 5692 indicates a small effect that amounts to $A(V) = 0.168$ (*total* extinction), corresponding to a total reddening of $E(B-V) = 0.054$. The maps by Burstein & Heiles (1982) give a similar value of $E(B-V) = 0.042$. We adopt the average of these two results, and after correction for the distance of HR 5692[8] we obtain $E(B-V) = 0.023 \pm 0.010$ and $A(V) = 3.1 \times E(B-V) = 0.071 \pm 0.031$. Independent support for a small degree of extinction is given by the polarization measurements of the star (Mathewson & Ford 1970; Leroy 1993, average polarization $p = 0.22 \pm 0.02\%$), which imply the presence of dust along the line of sight. The upper limit on the reddening that we infer from these measurements (see, e.g., Serkowski et al. 1975) is $E(B-V) \approx 0.024$, which happens to be close to the adopted estimate from dust maps. Applying this extinction correction leads to $M_V = 0.65 \pm 0.15$, in which the uncertainty is dominated by the parallax error.

[8] The correction is $E(B-V) = E(B-V)_{\rm tot}[1 - \exp(-D|\sin b|/H)]$, where $E(B-V)_{\rm tot}$ is the total reddening as derived from the dust maps, $E(B-V)$ is the reddening at distance D, b is the Galactic latitude, and H is the scale height of the dust layer, assumed here to be 125 pc (Marshall et al. 2006).

Table 4
Photometric Colors and Effective Temperatures for HR 5692

Photometric System	Color Index[a] (mag)	$T_{\rm eff}$[b] (K)
Johnson ($B-V$)	0.966 ± 0.007	4866 ± 57
Geneva (B_2-G)	0.456 ± 0.01	4850 ± 48
Geneva (B_2-V_1)	0.664 ± 0.01	4840 ± 56
Geneva (t) [c]	0.426 ± 0.02	4813 ± 72
DDO C(42−45)	0.830 ± 0.01	4848 ± 65
DDO C(42−48)	1.992 ± 0.01	4853 ± 56
2MASS ($V-J$)	1.405 ± 0.232	5372 ± 271
2MASS ($V-H$)	2.032 ± 0.196	5019 ± 225
2MASS ($V-K$)	2.094 ± 0.326	5027 ± 356
Tycho (B_T-V_T)	1.115 ± 0.017	4869 ± 87
Tycho–2MASS (V_T-K)	2.187 ± 0.326	5041 ± 344

Notes.
[a] Not corrected for reddening.
[b] Metallicity and reddening effects have been taken into account, and uncertainties include contributions from all sources (see the text).
[c] Defined as $t \equiv (B_2-G) - 0.39\,(B_1-B_2)$ (see Ramírez & Meléndez 2005).

In addition to our spectroscopic effective temperature estimate of $T_{\rm eff} = 4960 \pm 100$ K from Section 2, an independent determination was reported by Kovtyukh et al. (2006) as $T_{\rm eff} = 4995 \pm 6$ K based on the technique of line-depth ratios, although the formal uncertainty is almost certainly underestimated. Nevertheless, the value agrees with ours. Another $T_{\rm eff}$ estimate may be obtained from the large body of photometric measurements available for the star in a variety of standard systems, together with color–temperature calibrations. In Table 4, we have compiled a total of 11 optical and near-infrared color indices based on measurements in five different photometric systems (Johnson, Geneva, DDO, Tycho, and Two Micron All Sky Survey (2MASS); see Häggkvist & Oja 1987; Lu 1991; Mermilliod et al. 1997). We used the color–temperature calibrations for giants by Ramírez & Meléndez (2005) to estimate an effective temperature from each index. These calibrations include metallicity terms, for which we used the value [Fe/H] $= -0.21 \pm 0.05$, and all indices were corrected for reddening following Cardelli et al. (1989). The results are shown in Table 4, where the uncertainty in each temperature derivation includes contributions from the photometric errors, the scatter of the calibrations, and the uncertainties in both the metallicity and reddening. The various estimates show excellent agreement, the only discrepant value being that derived from $V-J$. We attribute this to an unexplained error in the 2MASS J magnitude of HR 5692. The remaining $T_{\rm eff}$ values are not independent of each other, but nevertheless convey a useful sense of the interagreement among the calibrations. The dispersion of these determinations is 88 K, and their weighted average is $T_{\rm eff} = 4852 \pm 22$ K, in which the formal error accounts for the different weights of the various measures as well as their scatter, but not potential systematic errors in the calibrations. Recently, Casagrande et al. (2010) have shown that the $T_{\rm eff}$ scale of Ramírez & Meléndez (2005) for dwarfs and subgiants is probably too low by roughly 100 K, which has to do with the infrared absolute flux calibrations adopted by Ramírez & Meléndez (2005). If this difference also applies to giants, which seems likely, a correction to our average photometric temperature for HR 5692 would bring it into excellent agreement with the spectroscopic value. The consistency of the three independent estimates described above (two spectroscopic, and one photometric) suggests the temperature of the star is accurately known, and we adopt in the following our spectroscopic result of $T_{\rm eff} = 4960 \pm 100$ K.

In estimating the mass of the primary of HR 5692 from a comparison of its $T_{\rm eff}$, M_V, and [Fe/H] values with stellar evolution models, an ambiguity arises because red giant stars in very different evolutionary stages can occupy the same region of the H-R diagram, for certain mass ranges. Specifically, stars on their first ascent of the giant branch and stars that are already burning helium in their cores after having experienced the helium flash ("clump giants") can have virtually the same temperature and luminosity. Masses inferred from models for these two states can differ by several tenths of a solar mass. Thus, another indicator is needed to discriminate between them. HR 5692 is bright enough that several detailed chemical abundance analyses are available including diagnostic signatures such as the lithium abundance and the C/N ratio. These two indices change drastically as stars evolve and experience the "first dredge-up." Clump giants around the mass expected for HR 5692 have Li abundances 50–100 times smaller than the primordial value of $\log N({\rm Li}) \approx 3.2$. Their typical C/N ratios have decreased from ∼3.3 on the main sequence to about 0.8, depending somewhat on mass and metallicity (see, e.g., Bertelli et al. 2008), due to mixing of the outer layers with matter from the interior partially processed through the CNO cycle. The Li abundance of HR 5692 has been measured by Brown et al. (1989) as $\log N({\rm Li}) = 1.3 \pm 0.3$, which is the same value reported independently by Mishenina et al. (2006) ($\log N({\rm Li}) = 1.30 \pm 0.15$). The latter authors also measured the C/H and N/H ratios, which lead to a C/N ratio of $1.07^{+0.67}_{-0.41}$. Both of these diagnostic indicators are thus quite typical of clump giants, so we conclude, as have others, that HR 5692 is indeed a core helium-burning star. This is also the most likely evolutionary state based on timescale arguments (clump status lasting much longer than other giant phases). We therefore restrict our model comparisons to stars in this phase.

Figure 6 shows an excellent fit between the observations for HR 5692 and an isochrone from the Padova series by Girardi et al. (2000), for a metallicity equal to the measured value of [Fe/H] $= -0.21$ and an age of 1.45 Gyr. The best-fitting mass is $M_{\rm RG} = 1.84\,M_\odot$. The uncertainty in this mass coming from the temperature and absolute magnitude errors is approximately $0.35\,M_\odot$. Errors in the chemical composition are also important as changes in metallicity shift the isochrones mostly horizontally in this diagram. We estimate the error contribution from this source to be $\sim 0.20\,M_\odot$. Adding both sources of error in quadrature we obtain the final mass estimate $M_{\rm RG} = 1.84 \pm 0.40\,M_\odot$. For this mass the models yield a luminosity of $\log L/L_\odot = 1.75$ and a surface gravity of $\log g = 2.68$. The latter agrees very well with our own spectroscopic estimate from Section 2 ($\log g = 2.67 \pm 0.20$) and with other determinations by Brown et al. (1989) and Mishenina et al. (2006) ($\log g = 2.7$ and 2.60, respectively). The predicted linear radius of the red giant is $R_{\rm RG} = 10.3\,R_\odot$, corresponding to an angular diameter of 0.97 mas at the distance of HR 5692.

The mass of the white dwarf then becomes $M_{\rm WD} = 0.59 \pm 0.12\,M_\odot$, where the uncertainty in the primary mass contributes slightly less ($0.078\,M_\odot$) than the uncertainty coming from the orbital elements and their correlations ($0.094\,M_\odot$). The physical properties of both stars are summarized in Table 5.

5. *IUE* SPECTRUM

HR 5692 was observed with the *IUE*, as part of a program to observe late-type stars with an ultraviolet excess in the TD-1

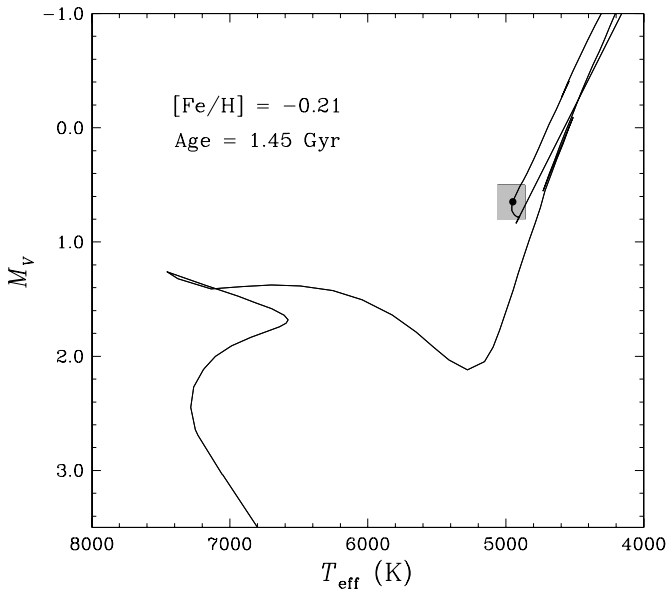

Figure 6. Location of HR 5692 in a diagram of absolute visual magnitude vs. effective temperature. The observational errors are represented by the shaded box. Overplotted is the best-fitting isochrone from the series by Girardi et al. (2000) corresponding to [Fe/H] = −0.21, with the star located in the core helium-burning clump. The nominal age of this isochrone is 1.45 Gyr, and the best-fitting mass is 1.84 $M_\odot$.

Table 5
Derived Physical Properties of the Components of HR 5692

Parameter	Value
Red giant primary	
$T_{\rm eff}$ (K)	4960 ± 100
M_V (mag)	0.65 ± 0.15
$M_{\rm RG}$ ($M_\odot$)	1.84 ± 0.40
$R_{\rm RG}$ ($R_\odot$)	10.3
log g	2.68
log $L/L_\odot$	1.75
White dwarf secondary	
$M_{\rm WD}$ ($M_\odot$)[a]	0.59 ± 0.12
$M_{\rm WD}$ ($M_\odot$)[b]	0.79 ± 0.09
$T_{\rm eff}$ (K)	30400 ± 780
log g	8.25 ± 0.15

Notes.
[a] Mass derived from the astrometric-spectroscopic orbital solution.
[b] Mass derived from the *IUE* spectrum analysis.

all-sky survey (Landsman et al. 1996). The ultraviolet excess of HR 5692 has since been recorded in the *Galaxy Evolution Explorer* (*GALEX*) All-Sky Imaging Survey (AIS; Martin et al. 2005). In the *GALEX* GR4 pipeline (Morrissey et al. 2007), the FUV magnitude of HR 5692 is given as 13.88. Though this magnitude is in the *GALEX* saturation regime, the derived flux of 1.32 $\times 10^{-13}$ erg cm^{-2} s^{-1} Å^{-1} at 1520 Å is in reasonable agreement with the *IUE* spectrum (Figure 1).

A 4200 s *IUE* spectrum (SWP 55294) of HR 5692 was obtained on 1995 August 7. A previous 1200 s spectrum (SWP 54718) obtained on 1995 May 20 was not used because the observing log indicated tracking errors, and the flux levels were down about 12% compared to the longer exposure. The processing of the *IUE* spectrum followed the prescriptions of Holberg et al. (2003) and, in particular, used the Massa & Fitzpatrick (2000) corrections to the NEWSIPS processed files. The presence of a hot white dwarf in HR 5692 is indicated

Table 6
White Dwarf Model Fits for $E(B-V) = 0.023$

log g	$T_{\rm eff}$ (K)	$R^2_{\rm WD}/d^2$	$M_{\rm WD}/M_\odot$	d (pc)
7.5	27,269	9.54×10^{-24}	0.422	141.0
7.75	28,404	8.35×10^{-24}	0.520	126.2
8.0	29,431	7.19×10^{-24}	0.644	112.0
8.25	30,485	6.43×10^{-24}	0.790	99.1
8.5	31,660	8.35×10^{-24}	0.944	86.2

by the broad Lyα absorption and rising continuum toward shorter wavelengths (Figure 1). The spectrum shows a possible weak emission feature shortward of 1548 Å which might be chromospheric C IV emission from the primary, consistent with HR 5692 being a coronal source (Jorissen et al. 1996). To avoid possible contamination from the primary, the analysis of the white dwarf spectrum is restricted to wavelengths shorter than 1500 Å.

As discussed by Landsman et al. (1996) and Burleigh et al. (1997), it is not possible to constrain both log g and $T_{\rm eff}$ with data solely from a low-dispersion *IUE* spectrum. However, one can construct a grid of ($T_{\rm eff}$, log g) values that fit the *IUE* spectrum, and then use the stellar distance, d, and a mass–radius relation to further constrain the white dwarf parameters. We computed a grid of pure hydrogen non-LTE model atmospheres using Version 204b of TLUSTY and Version 49 of Synspec (Lanz & Hubeny 1995) which includes the quasi-molecular satellites of Lyα and Lyβ. These models do not include the new Stark broadening calculations of Tremblay & Bergeron (2009). These new calculations generally yield higher derived masses for the case of Balmer line fits (Tremblay & Bergeron 2009), but further investigation is needed to determine the effect on fits to the Lyα line. For each assumed value of log g, Table 6 gives best-fit values of $T_{\rm eff}$ and $R^2_{\rm WD}/d^2$ required to match the model spectra to the *IUE* data. The model spectra were reddened assuming $E(B-V) = 0.023$ (Section 4), and the reddening curve of Cardelli et al. (1989).

We then use the carbon-core cooling models of Wood (1995) with thick hydrogen layers of q(H) = 10^{-4} and q(He) = 10^{-2} to provide a mass–radius relation, and derive distance and mass for each model fit given in Table 6. Interpolating in Table 6 using our revised *Hipparcos* distance $d = 98.8^{+7.0}_{-6.1}$ pc (Section 4) yields a mass of 0.80 ± 0.08 $M_\odot$. We repeated the mass determination many times in Monte Carlo simulations, which included a 0.01 mag uncertainty in the reddening, a 3% uncertainty in the *IUE* absolute calibration (Massa & Fitzpatrick 2000), and the uncertainty in the fitted $T_{\rm eff}$ and scale factor, along with the dominant parallax uncertainty. The derived values are log g = 8.25 ± 0.15, $T_{\rm eff}$ = 30,400 ± 780 K, and a mass of 0.79 ± 0.09 $M_\odot$. These white dwarf properties are summarized in Table 5.

In Figure 7, we show the *IUE* long-wavelength spectrum of the primary compared with a Kurucz model with our adopted stellar parameters of $T_{\rm eff}$ = 4960 K, log g = 2.7, and [Fe/H] = −0.21, and with models 100 K hotter and cooler. The models are normalized to V = 5.70, so there are no free parameters. Between 2900 and 3200 Å, the *IUE* spectrum falls slightly below the model spectrum. Since there is a tradeoff in the UV between $T_{\rm eff}$ and [Fe/H], one can get a better fit with either a temperature 100 K lower or with our adopted temperature and solar abundance. Given the uncertainty in our adopted parameters the agreement is reasonably good. In either case, the fit is less good at shorter wavelengths, likely due

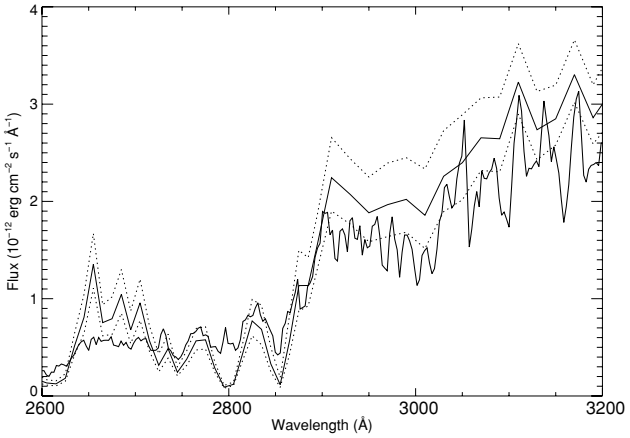

Figure 7. Long-wavelength *IUE* spectrum of HR 5692 (thick line) overlayed with a Kurucz model spectrum of the primary with $T_{\rm eff} = 4960$ K, $\log g = 2.7$, and [Fe/H] $= -0.21$ (thin line). The dotted lines show Kurucz models with $T_{\rm eff}$ set 100 K hotter and cooler.

to chromospheric Mg II, numerous near-UV metal lines poorly accounted for in the Kurucz models, and non-scaled abundances in the star.

6. DISCUSSION

The vast majority of white dwarf masses found in the literature depend on spectroscopic observations and models, such as spectroscopic determinations of the surface gravity using the profiles of Hydrogen lines, or the gravitational redshift, together with the parallax (see, e.g., Bergeron et al. 1992, 2007). There are a few white dwarf masses based on dynamical mass determinations which include the three famous white dwarfs in binaries that depend only on solutions for the absolute astrometric orbits: Sirius B (Gatewood & Gatewood 1978), Procyon B (Girard et al. 2000), and 40 Eri B (Heintz 1974). Recently, Parsons et al. (2010) reported on the white dwarf mass in the pre-cataclysmic binary NN Serpentis which is independent of any mass–radius relation. They also compiled, in their Figure 16, a few other white dwarfs in visual binaries and common proper-motion systems whose masses are also independent of any mass–radius relation.

As mentioned in Section 1, speckle interferometry by Mason et al. (1999) failed to resolve the system. The best-fit model to the white dwarf UV spectrum (Section 5) for this system predicts a white dwarf magnitude of about $V = 15.3$, yielding a magnitude difference between the primary and the white dwarf of 8.8 mag. The overwhelming brightness of the primary explains the null speckle result. Another potential method to resolve the binary is by *Hubble Space Telescope* (*HST*) imaging at UV wavelengths (≈2000 Å) where both the primary and secondary can be seen and the brightness of both components is similar. For example, Barstow et al. (2001) used this method to resolved several long-period late-type/white dwarf binaries, including the barium star Zet Cyg, for which they marginally resolve the white dwarf at a separation of 36 mas. Given an orbital radius of HR 5692 of $a_{\rm RG} = 4.14$ mas (Table 2), and a mass ratio of about three, we predict a maximum separation of 16.6 mas for the two components, which is likely unresolvable with *HST*.

We present two independent mass estimates for the white dwarf in the HR 5692 system: one based on an astrometric-spectroscopic orbital analysis ($0.59 \pm 0.12\,M_{\odot}$) and the other based on an analysis of an *IUE* spectrum ($0.79 \pm 0.09\,M_{\odot}$). The two estimates agree within 1σ error bars, but just barely. Both estimates are sensitive to the distance determination but that now seems to be relatively secure after including the *Hipparcos* intermediate astrometric data. The primary reasons that could account for the differences in our mass estimates are that the astrometric-spectroscopic mass is partly based on model isochrones that do not take into account any possible mass transfer that could cause deviations from single star evolution, and that the *IUE* spectrum analysis is based on the standard white dwarf mass–radius relation, which may not be appropriate. For example, the use of models from Wood (1995) with a negligible hydrogen surface layer would yield a mass about $0.05\,M_{\odot}$ lower than that derived in Section 5 using models with a thick hydrogen layer.

Although the fraction of white dwarfs that occur in binary systems may be as high as one-third (Holberg 2009), most of these are at sufficient separation that mass transfer to the companion star is insignificant and the post-main-sequence evolution leading to a white dwarf remnant is indistinguishable from that of an isolated star. The distribution of masses for isolated white dwarfs shows a relatively narrow peak at a value slightly below $0.6\,M_{\odot}$. However, this preferred mass value is not relevant for white dwarfs that form in close binaries, where mass transfer and orbital evolution are involved. In a simplified picture of that scenario, if the mass transfer is conservative then the orbit first shrinks on a rapid dynamical timescale until the mass of the evolving and donating star equals the mass of the receiving companion. After that the evolution of the orbit reverses and the separation grows more slowly, on a stellar-evolution timescale, since the mass transfer has to struggle to keep up with the expanding size of the Roche lobe. In an intriguing analysis of this scenario, Rappaport et al. (1995) suggest that the final size and period of the binary orbit are set by the end of mass transfer, when only the white dwarf cinder remains. Those authors present a theoretical model for estimating the orbital period versus mass of the white dwarf remnant.

In the case of HR 5692, the Rappaport et al. (1995) relation predicts that for the present orbital period of 506 days and eccentricity of 0.335, the corresponding mass of the remnant white dwarf should be in the range 0.33–0.44 $M_{\odot}$. However, this does not take into account subsequent mass transfer onto the white dwarf and orbital evolution that may have occurred as the star now seen as a clump giant evolved up the ascending giant branch and through the helium flash. The effect of that reverse mass transfer would be to increase the mass that we see now for the white dwarf. It would also shorten the orbital period, implying a larger mass for the white dwarf remnant at the end of its mass transfer to the original secondary. Both effects go in the direction of the larger mass now observed for the white dwarf.

If this scenario were true then the mass transfer raises questions about the assumption of using model isochrones based on single star evolution.

An alternative scenario is that of the binary evolution of barium stars. In this evolutionary scenario, the system starts out as a wide binary ($P > 10^3$ days) and the only mass transfer is through the asymptotic giant branch wind of the white dwarf progenitor and perhaps due to a "kick" of the white dwarf at birth (Izzard et al. 2010). The evolution of the companion (currently the giant star) would therefore closely resemble that of a single star, since the interaction is relatively weak. The evidence for HR 5692 being a barium star is ambiguous. Nevertheless, the significant eccentricity of the present orbit is consistent with this

scenario as mass transfer through other configurations involving Roche lobe overflow in a much tighter binary would most likely have circularized the orbit. Additionally, as we pointed out earlier, there is very good agreement between the measured surface gravity of the giant and the log g predicted from model isochrones for single-star evolution. The high temperature of the white dwarf implies that it is relatively young, and that the current primary may have already evolved off the main sequence when the white dwarf was born. The cooling models of Wood (1995) give an age of 24 Myr for a 0.8 $M_{\odot}$, 30,000 K white dwarf and an age of 10 Myr for a 0.6 $M_{\odot}$, 30,000 K white dwarf.

A detailed investigation of these proposed scenarios is warranted, but is beyond the scope of the present paper.

We thank Michael Calkins, Joe Caruso, Gil Esquerdo, and Joe Zajac for obtaining many of the spectroscopic observations used here. We also thank I. Hubeny for his assistance with the TLUSTY code. G.T. acknowledges partial support for this work from NSF grants AST-0708229 and AST-1007992. This research has made use of the SIMBAD database and the VizieR catalog access tool, both operated at CDS, Strasbourg, France, of NASA's Astrophysics Data System Abstract Service, and of data products from the Two Micron All Sky Survey (2MASS), which is a joint project of the University of Massachusetts and the Infrared Processing and Analysis Center/California Institute of Technology, funded by NASA and the NSF. Some of the data presented in this paper were obtained from the Multimission Archive at the Space Telescope Science Institute (MAST). STScI is operated by the Association of Universities for Research in Astronomy, Inc., under NASA contract NAS5-26555. Support for MAST for non-*HST* data is provided by the NASA Office of Space Science via grant NNX09AF08G and by other grants and contracts.

REFERENCES

Barstow, M. A., Bond, H. E., Burleigh, M. R., & Holberg, J. B. 2001, MNRAS, 322, 891
Bergeron, P., Gianninas, A., & Boudreault, S. 2007, in ASP Conf. Ser. 372, 15th European Workshop on White Dwarfs, ed. R. Napiwotzki & M. R. Burleigh (San Francisco, CA: ASP), 29
Bergeron, R., Saffer, A., & Liebert, J. 1992, ApJ, 394, 228
Bertelli, G., Girardi, L., Marigo, P., & Nasi, E. 2008, A&A, 484, 815
Brown, J. A., Sneden, C., Lambert, D. L., & Dutchover, E. 1989, ApJS, 71, 293
Burleigh, M. R., Barstow, M. A., & Fleming, T. A. 1997, MNRAS, 287, 381
Burstein, D., & Heiles, C. 1982, AJ, 87, 1165
Cardelli, J. A., Clayton, G. C., & Mathis, J. S. 1989, ApJ, 345, 245
Casagrande, L., Ramírez, I., Meléndez, J., Bessell, M., & Asplund, M. 2010, A&A, 512, 54
de Medeiros, J. R., & Mayor, M. 1999, A&AS, 139, 433
Frankowski, A., Jancart, S., & Jorissen, A. 2007, A&A, 464, 377
Gatewood, G. D., & Gatewood, C. V. 1978, ApJ, 225, 191
Girard, T. M., et al. 2000, AJ, 119, 2428
Girardi, L., Bressan, A., Bertelli, G., & Chiosi, C. 2000, A&AS, 141, 371
Griffin, R. 2009, The Observatory, 129, 6
Häggkvist, L., & Oja, T. 1987, A&AS, 68, 259
Heintz, W. D. 1974, AJ, 79, 819
Høg, E., et al. 2000, A&A, 355, L27
Holberg, J. B. 2009, J. Phys. Conf. Ser., 172, 2022
Holberg, J. B., Barstow, M. A., & Burleigh, M. R. 2003, ApJS, 147, 145
Izzard, R. G., Dermine, T., & Church, R. P. 2010, A&A, 523, A10
Jorissen, A., Schmitt, J. H. M. M., Carquillat, J. M., Ginestet, N., & Bickert, K. F. 1996, A&A, 306, 467
Kovtyukh, V. V., Soubiran, C., Bienaymé, O., Mishenina, T. V., & Belik, S. I. 2006, MNRAS, 371, 879
Kurtz, M. J., & Mink, D. J. 1998, PASP, 110, 934
Landsman, W., Simon, T., & Bergeron, P. 1996, PASP, 108, 250
Lanz, T., & Hubeny, I. 1995, ApJ, 439, 905
Latham, D. W. 1985, in IAU Colloq. 88, Stellar Radial Velocities, ed. A. G. D. Philip & D. W. Latham (Schenectady, NY: L. Davis Press), 21
Latham, D. W. 1992, in ASP Conf. Ser. 32, IAU Colloq. 135, Complementary Approaches to Binary and Multiple Star Research, ed. H. McAlister & W. Hartkopf (San Francisco, CA: ASP), 110
Leroy, J. L. 1993, A&A, 274, 203
Lu, P. K. 1991, AJ, 101, 2229
Makarov, V. V., & Kaplan, G. H. 2005, AJ, 129, 2420
Marshall, D. J., Robin, A. C., Reylé, C., Schultheis, M., & Picaud, S. 2006, A&A, 453, 635
Martin, D. C., et al. 2005, ApJ, 619, L1
Mason, B. D., et al. 1999, AJ, 117, 1890
Massa, D., & Fitzpatrick, E. L. 2000, ApJS, 126, 517
Massarotti, A., Latham, D. W., Stefanik, R. P., & Fogel, J. 2008, AJ, 135, 209
Mathewson, D. S., & Ford, V. L. 1970, MemRAS, 74, 139
McClure, R. D., & Woodsworth, A. W. 1990, ApJ, 352, 709
Mermilliod, J.-C., Hauck, B., & Mermilliod, M. 1997, A&AS, 124, 349
Mishenina, T. V., Bienayme, O., Gorbaneva, T. I., Charbonnel, C., Soubiran, C., Korotin, S. A., & Kovtyukh, V. V. 2006, A&A, 456, 1109
Morrissey, P., et al. 2007, ApJS, 173, 682
Nordström, B., Latham, D. W., Morse, J. A., Milone, A. A. E., Kurucz, R. L., Andersen, J., & Stefanik, R. P. 1994, A&A, 287, 338
Parsons, S. G., Marsh, T. R., Copperwheat, C. M., Dhillon, V. S., Littlefair, S. P., Gänsicke, B. T., & Hickman, R. 2010, MNRAS, 402, 2591
Perryman, M. A. C., & ESA, 1997, The *Hipparcos* and *Tycho* Catalogues (ESA SP-1200; Noordwijk: ESA)
Pourbaix, D., & Jorissen, A. 2000, A&AS, 145, 161
Press, W. H., Teukolsky, S. A., Vetterling, W. T., & Flannery, B. P. 1992, Numerical Recipes in FORTRAN (2nd. ed.; Cambridge: Cambridge Univ. Press), 650
Ramírez, I., & Meléndez, J. 2005, ApJ, 626, 465
Rappaport, S., Podsiadlowski, P., Joss, P. C., Di Stefano, R., & Han, Z. 1995, MNRAS, 273, 731
Schlegel, D. J., Finkbeiner, D. P., & Davis, M. 1998, ApJ, 500, 525
Serkowski, K., Mathewson, D. S., & Ford, V. L. 1975, ApJ, 196, 261
Torres, G. 2007, AJ, 133, 2684
Torres, G., Neuhäuser, R., & Guenther, E. W. 2002, AJ, 123, 1701
Tremblay, P., & Bergeron, P. 2009, ApJ, 696, 1755
van Leeuwen, F. 2007, Hipparcos, the New Reduction of the Raw Data (Astrophysics and Space Science Library, Vol. 350; Cambridge: Springer)
van Leeuwen, F., & Evans, D. W. 1998, A&AS, 130, 157
Wood, M. A. 1995, in White Dwarfs, ed. D. Koester & K. Werner (Lecture Notes in Physics, Vol. 443; Berlin: Springer), 41